

Communication

# 9,10-Bis[(4-(2-hydroxyethyl)piperazine-1-yl)prop-2-yn-1-yl]anthracene: Synthesis and G-Quadruplex Selectivity

Giovanni Ribaudo <sup>1,\*</sup>, Alberto Ongaro <sup>1</sup>, Erika Oselladore <sup>2</sup>, Giuseppe Zagotto <sup>2</sup>, Maurizio Memo <sup>1</sup> and Alessandra Gianoncelli <sup>1</sup>

<sup>1</sup> Department of Molecular and Translational Medicine, University of Brescia, 25121 Brescia, Italy; a.ongaro005@unibs.it (A.O.); maurizio.memo@unibs.it (M.M.); alessandra.gianoncelli@unibs.it (A.G.)

<sup>2</sup> Department of Pharmaceutical and Pharmacological Sciences, University of Padova, 35131 Padova, Italy; erika.oselladore@studenti.unipd.it (E.O.); giuseppe.zagotto@unipd.it (G.Z.)

\* Correspondence: giovanni.ribaudo@unibs.it; Tel.: +39-030-3717419

Received: 24 April 2020; Accepted: 20 May 2020; Published: 22 May 2020



**Abstract:** G-quadruplex DNA is the target of several natural and synthetic small molecules with antiproliferative and antiviral activity. We here report the synthesis through *Sonogashira* reaction and A3 coupling of a disubstituted anthracene derivative, 9,10-bis[(4-(2-hydroxyethyl)piperazine-1-yl)prop-2-yn-1-yl]anthracene. The binding of this compound to G-quadruplex and double stranded DNA sequences was evaluated using electrospray ionization mass spectrometry (ESI-MS), demonstrating selectivity for the first structure. The interaction pattern of the ligand with G-quadruplex was investigated by molecular docking and stacking was found to be the preferred binding mode.

**Keywords:** *Sonogashira* reaction; A3 coupling; anthracene; G-quadruplex; mass spectrometry; molecular modeling

## 1. Introduction

G-quadruplex DNA represents an attractive target for small molecules in the context of drug discovery [1–3]. These arrangements, constituted by stacked guanine nucleobases, can be formed by guanine-rich sequences, such as those that are present in telomeres, promoter genes and several viral genomes. The stabilization of G-quadruplexes with small ligands is a strategy for interfering with gene expression [4], uncontrolled cell proliferation [5] and viral replication [6–8].

Acridines, naphthalene diimides, anthracenes and anthraquinones are among the synthetic small molecules studied for their non-covalent interaction with double stranded DNA (dsDNA) and G-quadruplex structures [9–12]. More specifically, G-quadruplex ligands generally bear a planar scaffold and flexible side chains to efficiently bind the nucleic acid [13,14].

We previously presented a series of monosubstituted anthracene-propargylamine derivatives that were obtained through the A3 coupling reaction. Concerning DNA-binding properties, a set of electrospray ionization mass spectrometry (ESI-MS) experiments demonstrated a general preference for dsDNA over G-quadruplex and an overall lack of selectivity [15]. We here report the preparation of a novel disubstituted anthracene-propargylamine derivative through a multi-step approach and its preliminary evaluation as a G-quadruplex ligand by ESI-MS and molecular docking.

## 2. Results and Discussion

### 2.1. Chemistry

The target compound 9,10-bis[(4-(2-hydroxyethyl)piperazine-1-yl)prop-2-yn-1-yl]anthracene (**4**) was synthesized by a multi-step procedure starting from anthracene (Figure 1). This was selectively brominated in positions 9,10 with elemental bromine producing compound **1**. The resulting intermediate was subjected to a *Sonogashira* coupling reaction with trimethylsilylacetylene (TMS) on the two bromide atoms to insert the alkyne groups, giving compound **2**. These functions were then deprotected in basic conditions affording compound **3**. Analytical data were found in agreement with previous reports [16]. The final compound **4** was obtained from **3** by the copper-catalyzed A3 coupling reaction in the presence of formaldehyde and of the secondary amine 1-(2-hydroxyethyl)piperazine. Although the CuI coupling was previously reported on similar substrates, compound **4** is described here for the first time [17].

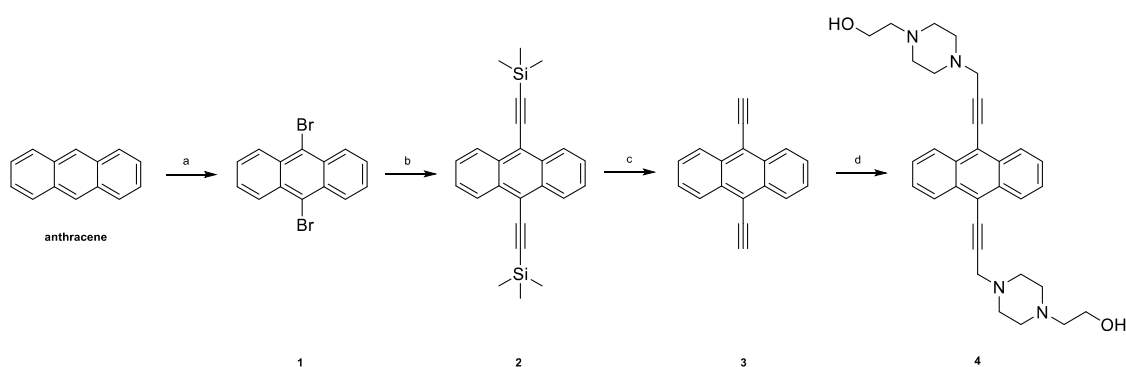


**Figure 1.** Synthetic scheme for the preparation of compound **4**. (a) Br<sub>2</sub>, CHCl<sub>3</sub>; (b) TMS, Pd(PPh<sub>3</sub>)<sub>4</sub>, CuI, TEA, toluene; (c) KOH, MeOH, THF; (d) HCOH, CuI, 1-(2-hydroxyethyl)piperazine, DMSO.

### 2.2. DNA Binding Studies

Analogous to our previous study on monosubstituted anthracenes [15], ESI-MS was used to evaluate the binding of compound **4** to a 23-mer containing the telomeric TTAGGG, a sequence that forms a monomeric G-quadruplex [13,18]. To investigate sequence selectivity, a dsDNA oligonucleotide was also introduced as control in the experimental design. The interaction efficiency was calculated in terms of binding affinity considering signal intensities in the mass spectra [18]. Compound **4** interacts with both DNA structures, but it preferentially binds G-quadruplex (see Figures S4 and S5 in the Supplementary material for mass spectra). In fact, as resumed in Table 1, a higher binding affinity value was recorded for the compound **4**/G-quadruplex complex. The results for **Ant4b**, the corresponding monosubstituted derivative that we demonstrated to be a non-selective dsDNA binder in our previous study, are also reported for comparison (see Figure S6 in the Supplementary material for chemical structures) [15]. A G-quadruplex/dsDNA selectivity ratio of 1.92 was calculated for compound **4**, demonstrating that the presence of two side chains in the scaffold turns the selectivity towards the first structure [19]. As we previously observed for the corresponding monosubstituted derivative, a 2:1 binding stoichiometry was detected [15].

**Table 1.** Results of the ESI-MS binding experiments and of the CID studies. Compound **Ant4b** was inserted as reference, since it represents the mono-substituted anthracene-propargylamine analogue of compound **4** (see Figure S5 in the Supplementary material for chemical structures) [15].  $E_{\text{COM}}^{50\%}$  values are expressed in eV.

Compound	Binding Affinity G-quadruplex	Binding Affinity dsDNA	Selectivity Ratio (G-quadruplex/dsDNA)	$E_{\text{COM}}^{50\%}$ 2:1 ligand/G-quadruplex	$E_{\text{COM}}^{50\%}$ 1:1 ligand/G-quadruplex	$E_{\text{COM}}^{50\%}$ 1:1 ligand/dsDNA
<b>4</b>	80.3	41.8	1.92	43.58	34.39	33.42
<b>Ant4b</b>	68.4	79.8	0.86	40.07	34.57	39.43

Collision-induced dissociation (CID) experiments were used to investigate the gas-phase relative kinetic stability of small molecule-DNA complexes ( $E_{\text{COM}}^{50\%}$ ), a parameter of biological relevance [2,20]. Dissociation by loss of the small molecule was observed and complex stability was evaluated by increasing collision energy (see Figures S7 and S8 in the Supplementary material) [20]. The results reported in Table 1 show that compound **4** efficiently stabilizes G-quadruplex in the 2:1 stoichiometry.

Based on sample concentration and relative peak intensities, ESI-MS can also be used to determine the equilibrium constants of complexes [13,21,22]. In particular, with respect to the complex formed by compound **4** with G-quadruplex,  $K_d = 0.69 \times 10^{-6}$  M was calculated under these experimental conditions [21–24]. The interaction pattern of compound **4** with the G-quadruplex structure, computed by molecular docking, is reported in Figure 2. Stacking was predicted as preferred binding motif and this result is in agreement with experimental observations suggesting that planar aromatic compounds preferentially interact with G-quadruplex in this manner [2,25].

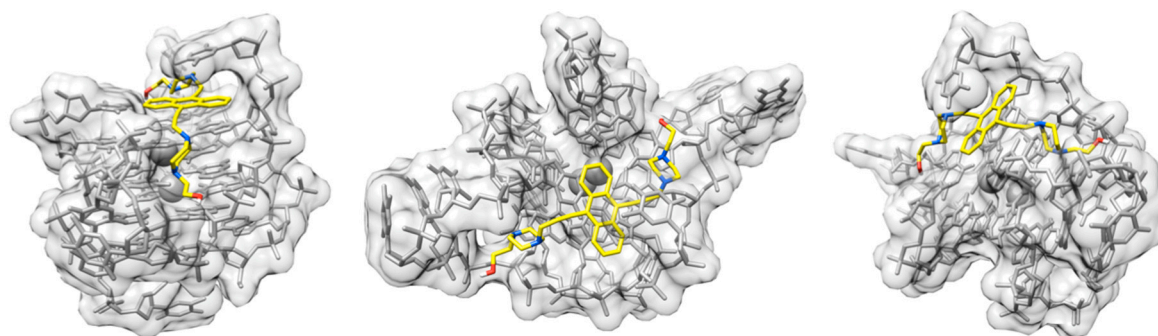


**Figure 2.** Predicted interaction pattern for compound **4** with G-quadruplex DNA (PDB ID: 3CE5), in three different views. Calculated binding energy: -8.5 kcal/mol.

### 3. Materials and Methods

#### 3.1. Chemistry

##### 3.1.1. General

Commercially available chemicals were purchased from Sigma-Aldrich (Saint Louis, MO, USA) and used as received, unless otherwise stated.  $^1\text{H}$  and  $^{13}\text{C}\{^1\text{H}\}$  NMR spectra were recorded on an Avance III 400 MHz spectrometer (Bruker, Billerica, MA, USA). All spectra were recorded at room temperature; the solvent for each spectrum is given in parentheses. Chemical shifts are reported in ppm and are relative to TMS internally referenced to the residual solvent peak. Datasets were edited with TopSpin (Bruker). The multiplicity of signals is reported as singlet (s), doublet (d), triplet (t), quartet (q), multiplet (m), broad (b), or a combination of any of these. Mass spectra were recorded by direct infusion ESI on LCQ Fleet (Thermo Fisher Scientific, Waltham, MA, USA) spectrometer. The purity profile (>96% unless otherwise stated) was assayed by HPLC using a Pro-Star system (Varian, Palo Alto, CA, USA) equipped with a 1706 UV-VIS detector (254 nm, Bio-rad, Hercules, CA, USA) and an C-18 column (5  $\mu\text{m}$ , 4.6  $\times$  250 mm, Agilent Technologies, Santa Clara, CA, USA).

An appropriate ratio of water (A) and acetonitrile (B) was used as mobile phase with an overall flow rate of 1 mL/min; the general method for the analyses is reported here: 0 min (95% A–5% B), 5 min (95% A–5% B), 15 min (5% A–95% B), 20 min (5% A–95% B), and 22 min (95% A–5% B).

### 3.1.2. Synthesis of 9,10-Dibromoanthracene (1)

Anthracene (4.5 g, 25.0 mmol) was dissolved in  $\text{CHCl}_3$  (50 mL) and a solution of bromine (3.0 mL, 58.2 mmol) in  $\text{CHCl}_3$  (25 mL) was added dropwise, inducing the formation of a solid precipitate. The mixture was stirred at r.t. for 4 h and afterwards the solvent was removed with a stream of  $\text{N}_2$ . The solid residue was triturated with DCM, filtered and washed with small portions of DCM to give **1** in yellow needles (4.1 g, 36%).  $^1\text{H-NMR}$  (400 MHz,  $\text{CDCl}_3$ ):  $\delta$  (ppm) = 8.57 (m, 4H), 7.62 (m, 4H),  $^{13}\text{C-NMR}$  (100 MHz,  $\text{CDCl}_3$ ):  $\delta$  (ppm) = 131.2, 128.4, 127.6, 123.7.

### 3.1.3. Synthesis of 9,10-Bis((trimethylsilyl)ethynyl)anthracene (2)

Compound **1** (236 mg, 0.70 mmol) and TMS were dissolved in a mixture of toluene (37.0 mL) and triethylamine (8.4 mL). Tetrakis(triphenyl-1-phosphine) palladium (17 mg, 0.015 mmol) and copper iodide (5.5 mg, 0.029 mmol) were then added. The mixture was purged with nitrogen and heated at reflux overnight. The solvent was removed at reduced pressure and the obtained mixture was poured in water and extracted with DCM, dried over anhydrous magnesium sulphate and evaporated under reduced pressure. The crude product was purified by column chromatography (silica gel, hexane) obtaining compound **2** as a red solid (86 mg, 36%).  $^1\text{H-NMR}$  (400 MHz,  $\text{CDCl}_3$ ):  $\delta$  (ppm) = 8.61 (m, 4H), 7.63 (m, 4H), 0.47 (s, 18H),  $^{13}\text{C-NMR}$  (100 MHz,  $\text{CDCl}_3$ ):  $\delta$  (ppm) = 132.1, 127.2, 126.4, 117.5, 108.3, 101.7, 0.2.

### 3.1.4. Synthesis of 9,10-Diethynylantracene (3)

Compound **2** (80 mg, 0.22 mmol) was dissolved in a mixture of MeOH (6.4 mL) and THF (3.2 mL), and 10% KOH was then added (1.2 mL). The solution was stirred at r.t. for 3 h and then the solvent was partially evaporated under reduced pressure. After that, diethyl ether (20 mL) was added, the obtained mixture was washed with water ( $3 \times 10$  mL), dried over magnesium sulphate and evaporated under reduced pressure obtaining a grey solid (45 mg, 91%).  $^1\text{H-NMR}$  (400 MHz,  $\text{CDCl}_3$ ):  $\delta$  (ppm) = 8.61 (m, 4H), 7.62 (m, 4H), 4.07 (s, 2H),  $^{13}\text{C-NMR}$  (100 MHz,  $\text{CDCl}_3$ ):  $\delta$  (ppm) = 132.5, 127.2, 127.10, 117.5, 90.1, 80.3.

### 3.1.5. Synthesis of 9,10-Bis[(4-(2-hydroxyethyl)piperazine-1-yl)prop-2-yne-1-yl]anthracene (4)

Compound **3** (45 mg, 0.2 mmol), 37% formaldehyde (200  $\mu\text{L}$ , 2.5 mmol), copper iodide (7 mg, 0.04 mmol) and 1-(2-Hydroxyethyl)piperazine (80 mg, 0.6 mmol) were dissolved in DMSO (1 mL). The solution was stirred overnight at r.t. and then DCM (30 mL) was added. The resulting mixture was washed with 0.1 M KOH ( $4 \times 10$  mL). The crude product was purified by column chromatography (silica gel, gradient of MeOH/TEA/DCM from 2,5/0,75/96,75 to 10/2/88) obtaining a solid yellow product (25 mg, 25%).  $^1\text{H-NMR}$  (400 MHz, d-DMSO):  $\delta$  (ppm) = 8.54 (m, 4H), 7.74 (m, 4H), 4.36 (t, 2H,  $J = 5.4$  Hz), 3.90 (s, 4H), 3.50 (m, 4H), 2.72 (bs, 8H), 2.51 (bs, 8H), 2.41 (t, 4H,  $J = 6.2$  Hz),  $^{13}\text{C-NMR}$  (100 MHz,  $\text{CDCl}_3$ ):  $\delta$  (ppm) = 132.8, 128.7, 127.2, 117.0, 95.4, 82.2, 59.5, 55.4, 52.9, 51.6, 48.2. ESI-MS: found 511.04 ( $\text{C}_{32}\text{H}_{39}\text{N}_4\text{O}_2^+$ ,  $[\text{M} + \text{H}]^+$ ), calc. 511.31.

## 3.2. ESI-MS Binding Studies

DNA sequences were obtained from Sigma-Aldrich (Saint Louis, MO, USA). Samples were heat-denatured and folded in 150 mM ammonium acetate before incubation with the ligand; ligand stock solution was prepared in methanol. The final concentration of the oligonucleotide was 5–10  $\mu\text{M}$  in 150 mM ammonium acetate, with a 10:1 compound/oligo ratio. Samples were acquired after an equilibration time of 30 min and methanol was added to obtain a stable ESI

signal. Mass spectra were recorded by direct infusion. The instrument was set in negative ionization mode with a 3.4 kV capillary voltage, 120 °C capillary temperature and a flow rate of 5 µL/min. Collision-induced dissociation (CID) experiments were performed on the complexes by isolating the precursor ion in the trap and increasing the “normalized collision energy” parameter. Exact mass for the G-quadruplex sequence (5′-AGGGTTAGGGTTAGGGTTAGGGT-3′): 7270.774 Da. Exact mass for dsDNA (5′-ACTATTTACGTATAATGA-3′, 5′-TCATTATACGTAAATAGT-3′): 10987.922 Da. Exact mass for 9,10-bis[(4-(2-hydroxyethyl)piperazine-1-yl)prop-2-yn-1-yl]anthracene (**4**): 510.299 Da. Binding affinity was calculated according to the formula:  $BA = (\Sigma DNA_{bound} / (\Sigma DNA_{free} + \Sigma DNA_{bound})) \times 100$  [18,26]. In CID studies, relative intensity (%) of the DNA/ligand signal was plotted against the applied energy expressed in eV (logarithmic scale). Relative I (%) =  $(I_{complex} / (I_{complex} + I_{dissociation\ products})) \times 100$  [27]. To determine the equilibrium constant of compound **4**/G-quadruplex complex, the following calculations were considered:  $[ligand]_{bound} = n[DNA]_0[ligand]/(K_d + [ligand])$ ,  $[complex] = C_0 \times I_{complex}/(I_{complex} + I_{DNA})$ ,  $[ligand] = C_0 - n[complex]$  [21–24].

### 3.3. Molecular Modeling

The structure of the macromolecular target was obtained from the RCSB Protein Data Bank ([www.rcsb.org](http://www.rcsb.org), PDB ID: 3CE5). Target and ligand were prepared for the blind docking experiment which was performed using Autodock Vina (Molecular Graphics Laboratory, Department of Integrative Structural and Computational Biology, The Scripps Research Institute, La Jolla, CA, USA) [28]. Output data (energies, interaction patterns) were analyzed and scored using UCSF Chimera molecular viewer [29], which was also used to produce the artworks.

## 4. Conclusions

We reported the preparation of a disubstituted anthracene-propargylamine derivative through a multi-step approach. Compound **4** showed improved selectivity towards G-quadruplex over dsDNA with respect to the monosubstituted analogue in the ESI-MS binding experiment and in the CID study. This may due to the fact that the disubstituted anthracene derivative has a lower tendency to interact with dsDNA through intercalation, due to steric hindrance. At the same time, the presence of a second side chain on the molecule allows the ligand to generate more efficient non-covalent interactions with G-quadruplex DNA, as observed in the pattern predicted by docking studies. Compound **4** represents a first-in-class compound that paves the way for the development of other selective G-quadruplex binders.

**Supplementary Materials:** The following are available online, Figures S1 and S2: NMR spectra, Figure S3: ESI-MS spectrum, Figures S4 and S5: ESI-MS spectra (binding studies), Figure S6: chemical structures, Figure S7: ESI-MS spectrum (CID fragmentation), Figure S8: CID fragmentation curves.

**Author Contributions:** Conceptualization, G.R. and A.G.; methodology, G.R.; software, A.O. and G.R.; investigation, A.O., E.O. and G.R.; data curation, G.R.; writing—original draft preparation, G.R., A.O. and A.G.; writing—review and editing, M.M. and G.Z.; supervision, G.R. and A.G.; funding acquisition, A.G. All authors have read and agreed to the published version of the manuscript.

**Funding:** This research was granted by University of Brescia.

**Conflicts of Interest:** The authors declare no conflict of interest.

## References

- Altieri, A.; Alvino, A.; Ohnmacht, S.; Ortaggi, G.; Neidle, S.; Nocioni, D.; Franceschin, M.; Bianco, A. Xanthene and Xanthone Derivatives as G-Quadruplex Stabilizing Ligands. *Molecules* **2013**, *18*, 13446–13470. [[CrossRef](#)] [[PubMed](#)]
- Ribaudo, G.; Ongaro, A.; Zagotto, G.; Memo, M.; Gianoncelli, A. Evidence on selective binding to G-quadruplex DNA of isoflavones from *Maclura pomifera* by mass spectrometry and molecular docking. *Nat. Prod. Res.* **2019**, 1–5. [[CrossRef](#)]

3. Ribaud, G.; Ongaro, A.; Zagotto, G.; Memo, M.; Gianoncelli, A. Photoactivated semi-synthetic derivative of osajin selectively interacts with G-quadruplex DNA. *Nat. Prod. Res.* **2020**, 1–6. [\[CrossRef\]](#)
4. Asamitsu, S.; Bando, T.; Sugiyama, H. Ligand Design to Acquire Specificity to Intended G-Quadruplex Structures. *Chem. A Eur. J.* **2019**, 25, 417–430. [\[CrossRef\]](#)
5. Rigo, R.; Palumbo, M.; Sissi, C. G-quadruplexes in human promoters: A challenge for therapeutic applications. *Biochim. Biophys. Acta Gen. Subj.* **2017**, 1861, 1399–1413. [\[CrossRef\]](#)
6. Chang, Y.-S.; Ko, B.-H.; Ju, J.-C.; Chang, H.-H.; Huang, S.-H.; Lin, C.-W. SARS Unique Domain (SUD) of Severe Acute Respiratory Syndrome Coronavirus Induces NLRP3 Inflammasome-Dependent CXCL10-Mediated Pulmonary Inflammation. *Int. J. Mol. Sci.* **2020**, 21, 3179. [\[CrossRef\]](#)
7. Shen, L.-W.; Qian, M.-Q.; Yu, K.; Narva, S.; Yu, F.; Wu, Y.-L.; Zhang, W. Inhibition of Influenza A virus propagation by benzoselenoxanthenes stabilizing TMPRSS2 Gene G-quadruplex and hence down-regulating TMPRSS2 expression. *Sci. Rep.* **2020**, 10, 7635. [\[CrossRef\]](#)
8. Di Fonzo, S.; Amato, J.; D'Aria, F.; Caterino, M.; D'Amico, F.; Gessini, A.; Brady, J.W.; Cesàro, A.; Pagano, B.; Giancola, C. Ligand binding to G-quadruplex DNA: New insights from ultraviolet resonance Raman spectroscopy. *Phys. Chem. Chem. Phys.* **2020**, 22, 8128–8140. [\[CrossRef\]](#)
9. Sengupta, A.; Ganguly, A.; Chowdhury, S. Promise of G-Quadruplex Structure Binding Ligands as Epigenetic Modifiers with Anti-Cancer Effects. *Molecules* **2019**, 24, 582. [\[CrossRef\]](#)
10. Pirota, V.; Nadai, M.; Doria, F.; Richter, S. Naphthalene Diimides as Multimodal G-Quadruplex-Selective Ligands. *Molecules* **2019**, 24, 426. [\[CrossRef\]](#)
11. Bortolus, M.; Ribaud, G.; Toffoletti, A.; Carbonera, D.; Zagotto, G. Photo-induced spin switching in a modified anthraquinone modulated by DNA binding. *Photochem. Photobiol. Sci.* **2019**, 18, 2199–2207. [\[CrossRef\]](#) [\[PubMed\]](#)
12. Ongaro, A.; Ribaud, G.; Braud, E.; Ethève-Quelquejeu, M.; De Franco, M.; Garbay, C.; Demange, L.; Gresh, N.; Zagotto, G. Design and synthesis of a peptide derivative of ametantrone targeting the major groove of the d(GGCGCC)<sub>2</sub> palindromic sequence. *New J. Chem.* **2020**, 44, 3624–3631. [\[CrossRef\]](#)
13. Ribaud, G.; Scalabrin, M.; Pavan, V.; Fabris, D.; Zagotto, G. Constrained bisantrene derivatives as G-quadruplex binders. *ARKIVOC* **2016**, 2016, 145.
14. Chilka, P.; Desai, N.; Datta, B. Small Molecule Fluorescent Probes for G-Quadruplex Visualization as Potential Cancer Theranostic Agents. *Molecules* **2019**, 24, 752. [\[CrossRef\]](#)
15. Ongaro, A.; Ribaud, G.; Zagotto, G.; Memo, M.; Gianoncelli, A. Synthesis via A3 Coupling Reaction of Anthracene-Propargylamine as a New Scaffold for the Interaction with DNA. *ChemistrySelect* **2019**, 4, 13138–13142. [\[CrossRef\]](#)
16. Zhu, J.; Zhong, K.; Liang, Y.; Wang, Z.; Chen, T.; Jin, L.Y. Synthesis and self-assembly of oligomers containing cruciform 9,10-bis(arylethynyl)anthracene unit: formation of supramolecular nanostructures based on rod-length-dependent organization. *Tetrahedron* **2014**, 70, 1230–1235. [\[CrossRef\]](#)
17. Zhang, C.-H.; Yu, P.-P.; Tan, W.-Y.; Luo, D.; Wang, L.-P.; Xia, Y.; Liu, C.-C.; Cao, Y. An easily and environmentally friendly accessible small-molecule acetylenic donor for organic solar cells. *Dye. Pigment.* **2019**, 160, 983–988. [\[CrossRef\]](#)
18. Ferreira, R.; Marchand, A.; Gabelica, V. Mass spectrometry and ion mobility spectrometry of G-quadruplexes. A study of solvent effects on dimer formation and structural transitions in the telomeric DNA sequence d(TAGGGTTAGGGT). *Methods* **2012**, 57, 56–63. [\[CrossRef\]](#)
19. Mazzitelli, C.L.; Brodbelt, J.S.; Kern, J.T.; Rodriguez, M.; Kerwin, S.M. Evaluation of binding of perylene diimide and benzannulated perylene diimide ligands to dna by electrospray ionization mass spectrometry. *J. Am. Soc. Mass Spectrom.* **2006**, 17, 593–604. [\[CrossRef\]](#)
20. Xu, N.; Yang, H.; Cui, M.; Song, F.; Liu, Z.; Liu, S. Evaluation of alkaloids binding to the parallel quadruplex structure [d(TGGGGT)]<sub>4</sub> by electrospray ionization mass spectrometry. *J. Mass Spectrom.* **2012**, 47, 694–700. [\[CrossRef\]](#)
21. Rosu, F. Determination of affinity, stoichiometry and sequence selectivity of minor groove binder complexes with double-stranded oligodeoxynucleotides by electrospray ionization mass spectrometry. *Nucleic Acids Res.* **2002**, 30, e82. [\[CrossRef\]](#)
22. Tjernberg, A.; Carnö, S.; Oliv, F.; Benkestock, K.; Edlund, P.-O.; Griffiths, W.J.; Hallén, D. Determination of Dissociation Constants for Protein–Ligand Complexes by Electrospray Ionization Mass Spectrometry. *Anal. Chem.* **2004**, 76, 4325–4331. [\[CrossRef\]](#)



23. Erba, E.B.; Zenobi, R. Mass spectrometric studies of dissociation constants of noncovalent complexes. *Annu. Reports Sect. "C" (Physical Chem.)* **2011**, *107*, 199–228. [[CrossRef](#)]
24. Ishii, K.; Noda, M.; Uchiyama, S. Mass spectrometric analysis of protein–ligand interactions. *Biophys. Physicobiology* **2016**, *13*, 87–95. [[CrossRef](#)]
25. Tawani, A.; Kumar, A. Structural Insight into the interaction of Flavonoids with Human Telomeric Sequence. *Sci. Rep.* **2015**, *5*, 17574. [[CrossRef](#)]
26. Ribaud, G.; Ongaro, A.; Zorzan, M.; Pezzani, R.; Redaelli, M.; Zagotto, G.; Memo, M.; Gianoncelli, A. Investigation of the molecular reactivity of bioactive oxiranylmethoxy anthraquinones. *Arch. Pharm. (Weinheim)* **2019**, *352*, 1900030. [[CrossRef](#)]
27. Torvinen, M.; Kalenius, E.; Sansone, F.; Casnati, A.; Jänis, J. Noncovalent Complexation of Monoamine Neurotransmitters and Related Ammonium Ions by Tetramethoxy Tetraglucosylcalix [4]arene. *J. Am. Soc. Mass Spectrom.* **2012**, *23*, 359–365. [[CrossRef](#)]
28. Trott, O.; Olson, A.J. AutoDock Vina: Improving the speed and accuracy of docking with a new scoring function, efficient optimization, and multithreading. *J. Comput. Chem.* **2010**, *31*, 455–461. [[CrossRef](#)]
29. Pettersen, E.F.; Goddard, T.D.; Huang, C.C.; Couch, G.S.; Greenblatt, D.M.; Meng, E.C.; Ferrin, T.E. UCSF Chimera - A visualization system for exploratory research and analysis. *J. Comput. Chem.* **2004**, *25*, 1605–1612. [[CrossRef](#)]



© 2020 by the authors. Licensee MDPI, Basel, Switzerland. This article is an open access article distributed under the terms and conditions of the Creative Commons Attribution (CC BY) license (<http://creativecommons.org/licenses/by/4.0/>).